J. Pharm. Pharmac., 1966, **18**, 429–442 Received January 18, 1966

The flow of granular magnesia

T. M. JONES AND N. PILPEL

Investigations of the flow rates of loosely packed magnesia have shown that the general equation developed by Jones & Pilpel (1966)

$$D_o = A\left(\frac{4W}{60\pi\rho_p\sqrt{g}}\right)^{\frac{1}{n}}$$

can be applied to single component and multicomponent mixtures in the size range 0·003 to >0·2 cm. The increase in flow rate caused by mixing coarse and fine particles has been related quantitatively to the size of the particles by the general expression

$$\log \max = -[f(D_{Pc}.D_{Pf})]\, D_o + f(D_{Pc}.D_{Pf})$$

This can be used to calculate the composition for maximum flow in multicomponent mixtures. The mechanism of action of glidants is discussed in the light of the experimental results and a distinction is made between glidants which improve the flow of granulations and those which improve the flow of cohesive powders.

ALTHOUGH there have been many reports on the gravity flow of non-cohesive granular solids, little information is available about the gravity flow of particulate systems in which interparticular forces are operating.

Publications concerned with the improvement of flow of granulations by the addition of fine material (Hammerness & Thompson, 1958; Tucker & Hays, 1959; Fairs, 1960; Vegan, 1960; Gunsel & Lachman, 1963; Krishna & Rao, 1963; Bulsara, Zenz & Eckert, 1964), the addition of glidants to the powders (Munzel & Kagi, 1954; Craik & Miller, 1958) or admixture of coarse particles with powders (Davis, 1943; Hawkesley, 1947; Shotton & Simons, 1950; Nakajima, 1961) to improve their flow characteristics, have been mainly qualitative or comparative. The additives have often had very different chemical and physical properties to the main components; this has made it difficult to elucidate the basic mechanisms of their action.

We have examined the flow characteristics of single component and of multicomponent mixtures of granulated magnesia through circular orifices in order to extend the applicability of a previously developed flow equation (Jones & Pilpel, 1966) to the wider size range 0·003 to 0·3 cm, thus taking into account the effects of interparticular forces which occur when the particles are less than about 0·01 cm in diameter.

By investigating the effects of added fine material on the flow behaviour of coarser granules, it was hoped to gain a clearer understanding of the mechanisms of glidant action. We also hoped to be able to predict how much fine material should be added to a multicomponent mixture of coarser magnesia to increase its flow rate to a maximum.

Experimental

The experimental work consisted of measuring the flow rates of 13 single and 189 multicomponent mixtures of granulated magnesia through

From the School of Pharmacy, Chelsea College of Science and Technology, Manresa Road, London, S.W.3.

6 circular orifices from a vertical hopper with a horizontal base. The procedure already reported in detail by Jones & Pilpel (1966) was followed using the same batch of magnesia, particular care being taken to ensure that before the flow started the bed was at its loosest state of packing. Although flow rate is independent of initial voidage for non-cohesive materials, preliminary investigations indicated that the state of packing of the fine fractions had a pronounced effect on flow rate until the bed was fully dilated.

Angles of repose were determined after consolidating the samples. The apparatus used (Fig. 1) consisted of a box constructed with three

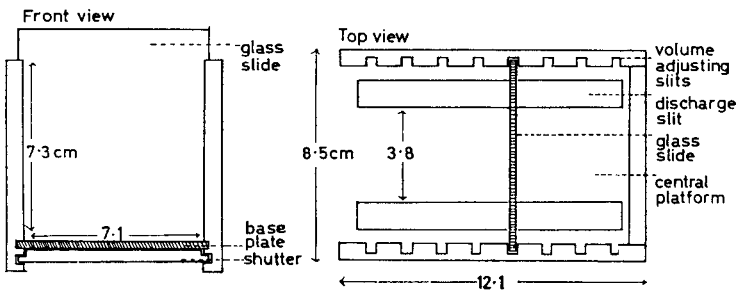

FIG. 1. Apparatus for measurement of consolidated angle of repose.

sides of wood and a laminated plastic base into which two parallel slits had been cut leaving a central platform 3·8 cm wide. The fourth side of the box was a glass slide, the position of which could be adjusted, thereby enabling the volume of the box to be varied.

The technique adopted was to insert a sliding shutter into the base of the box and then pour in the sample from a sheet of demy paper held 2 cm above the box. The bed was then consolidated by dropping the box 50 times from a height of 3 cm on to a flat surface, turning through 90° after each 10 drops. After careful removal of the shutter, the height of the wedge formed was measured and the consolidated angle of repose, θ, calculated from the expression $\tan \theta = 2h/L$ where h is the height of wedge and L, the width of platform.

Results

Fig. 2 shows the effect on the flow rates of coarse sieve fractions (D_{P_c} = 0·0561, 0·0253 cm) when varying concentrations of fine fractions (D_{P_f} = 0·0090, 0·0071 and 0·0048 cm) are added.

It is seen that the flow rate reaches a maximum at a particular concentration of fine material. The position of the maximum is dependent upon the size of both the fine and the coarse component.

Fig. 3 shows that the positions of these maxima vary with the diameter of the orifice, the concentration of fine material necessary to produce the maxima decreasing with increase in orifice diameter.

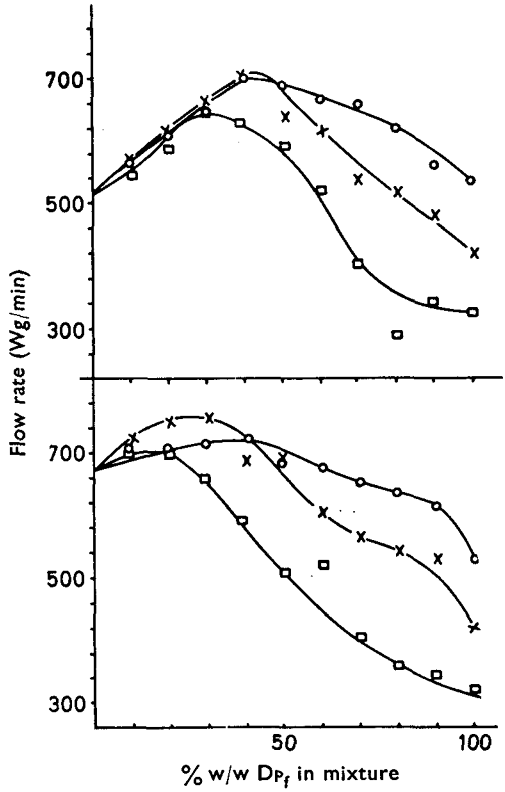

FIG. 2. The effect of particle size on flow rate of binary mixtures of coarse and fine components through a circular orifice D_o = 0·898 cm. D_{P_c} in top graph = 0·0561 cm and in bottom graph = 0·0253 cm. D_{P_f} = 0·0048 cm (□), 0·0071 cm (×) and 0·0090 cm (○).

Figs 4 (a–d) are representative ternary diagrams showing the variation in flow rate that occurs on the addition of a 3rd (coarse) component to an existing binary mixture of coarse and fine material.

Here too the positions of the maxima depend upon the size of the fine component—D_{P_f} Fig. 4 (a and c), the coarse component Fig. 4 (a and d), the orifice diameter Fig. 4 (a and b) and on the percentage of 3rd (coarse) component present Fig. 4 (a–d).

Discussion

GENERAL FLOW EQUATION

To extend the applicability of the previously developed equation (Jones & Pilpel, 1966),

$$D_o = A\left(\frac{4W}{60\pi\rho_P\sqrt{g}}\right)^{\frac{1}{n}} \quad \ldots \quad \ldots \quad \ldots \quad (1)$$

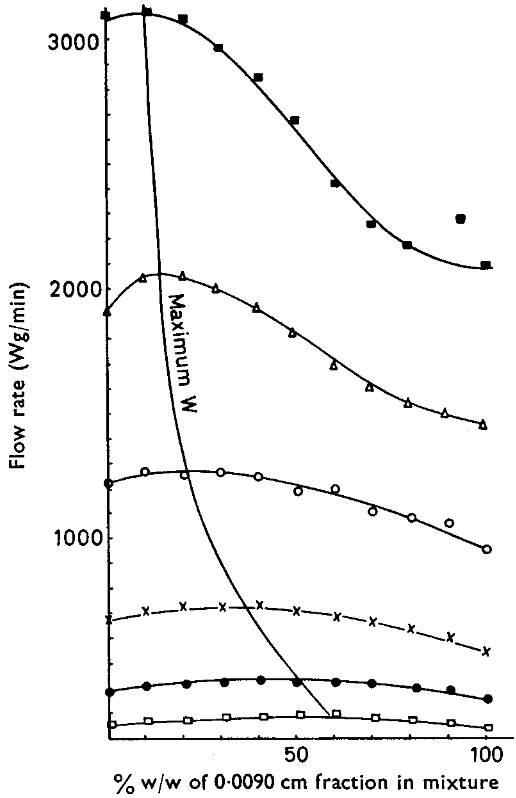

FIG. 3. Effect of orifice diameter on the flow rate of the binary mixture $D_{P_c} = 0{\cdot}0253$ cm, $D_{P_f} = 0{\cdot}0090$ cm. D_o in cm: ■ = 1·686, △ = 1·353, ○ = 1·140, × = 0·898 ● = 0·740, □ = 0·603.

where A and 1/n are functions of particle size, for predicting the flow rate of magnesia over the whole size range 0·003 to 0·3 cm, it is necessary to distinguish between four regions according to the size of the particles concerned.

In region I (particles >0·02 cm) magnesia is non-cohesive and free flowing due to the interparticular forces being ⩽ gravitational forces; the equation

$$D_o = (1{\cdot}6822\, D_{P_{av}} + 1{\cdot}9779)\left(\frac{4W}{60\pi\rho_P\sqrt{g}}\right)^{0{\cdot}2571 - 0{\cdot}0855 \log D_{P_{av}}} \text{applies.} \quad (2)$$

Region II ($0{\cdot}02 > D_p > 0{\cdot}01$ cm) represents a transition between region I and region III. Here the flow is beginning to be affected by interparticular forces of friction and cohesion. This can be seen for example by comparing the angle of repose of different sieve cuts of magnesia after consolidation, which causes the particles to pack closely, thereby accentuating the effect of interparticular forces. It is seen from Table 1 that changes in the angle of repose are most apparent in region II.

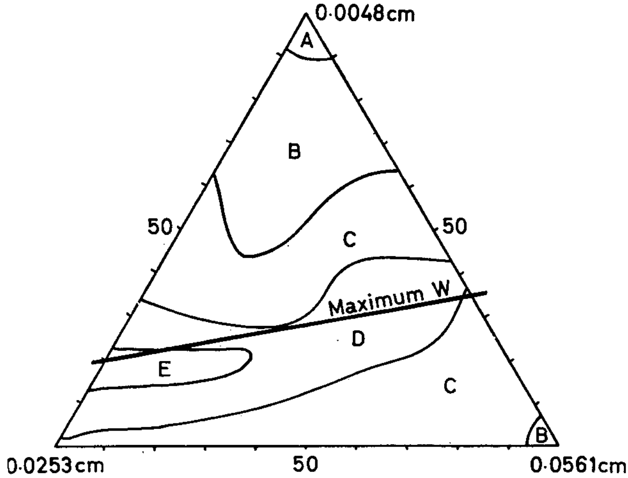

FIG. 4a. Flow contours for ternary system $D_{P_{c_1}}$ = 0·0561 cm, $D_{P_{c_2}}$ = 0·0253 cm, D_{P_f} = 0·0048 cm. D_o = 0·74 cm. Flow rate (W g/min): A = <200, B = 200–300, C = 300–400, D = 400–420, E = >420.

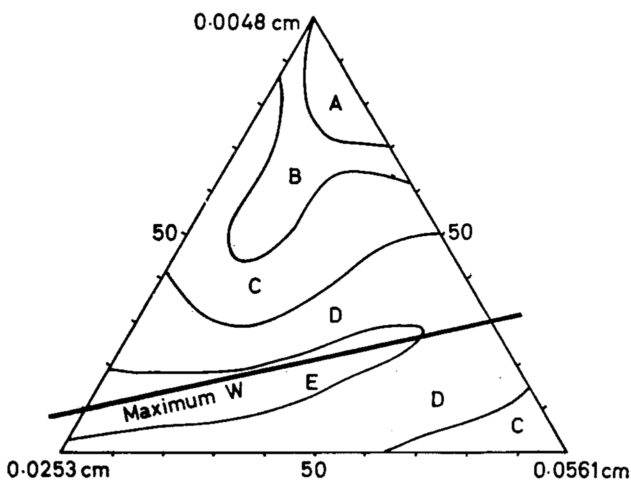

FIG. 4b. Flow contours for ternary system $D_{P_{c_1}}$ = 0·0561 cm, $D_{P_{c_2}}$ = 0·0253 cm, D_{P_f} = 0·0048 cm. D_o = 0·898 cm. Flow rate (W g/min): A = <400, B = 400–500, C = 500–600, D = 600–700, E = >700.

Region III covers particles from 0·003 to 0·01 cm. Here the forces between the particles are $\geqslant$ gravitational forces, the flow is still free. Finally in region IV where the particles are <0·003 cm, the predominant interparticular forces are of the van der Waals' type and are $\gg$ gravitational forces; the powder becomes "cohesive". Flow in this region can only be investigated by employing special techniques (Dawes, 1952; Jenike, 1961; Lowes & Perry, 1965) and we do not propose to discuss it further here.

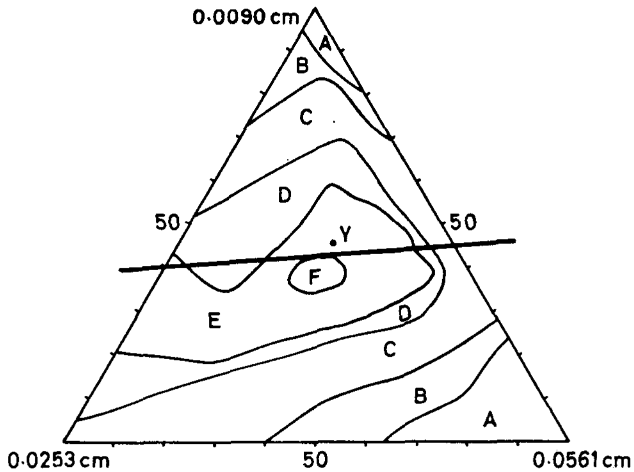

FIG. 4c. Flow contours for ternary system $D_{P_{c_1}}$ = 0·0561 cm, $D_{P_{c_2}}$ = 0·0253 cm, D_{P_f} = 0·0090 cm. D_o = 0·898 cm. Flow rate (W g/min): A = <600, B = 600–650, C = 650–700, D = 700–720, E = 720–730, F = >730.

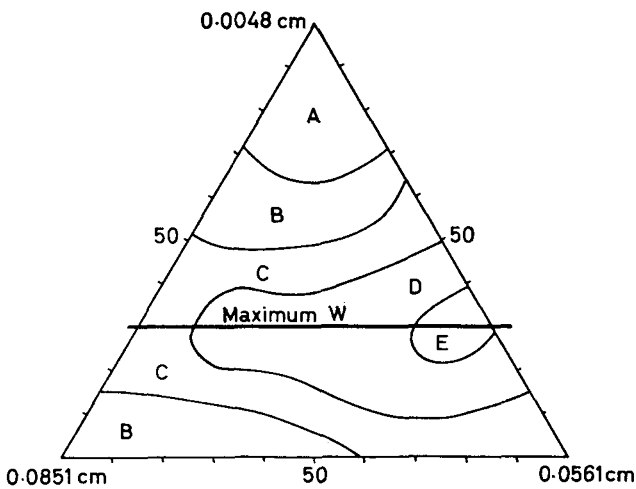

FIG. 4d. Flow contours for ternary system $D_{P_{c_1}}$ = 0·0561 cm, $D_{P_{c_2}}$ = 0·0851 cm, D_{P_f} = 0·0048 cm. D_o = 0·898 cm. Flow rate (W g/min): A = <400, B = 400–500, C = 500–600, D = 600–640, E = >640.

We can employ a similar treatment to that used in the previous paper (Jones & Pilpel, 1966) for evaluating the quantities A and 1/n for each region in terms of D_P or $D_{P_{av}}$ (the geometric mean diameter) where mixtures of particle sizes are being considered.

As A is essentially a measure of the forces between the particles, it varies in different ways with D_P from region to region. It is not therefore considered that a single expression relating A to D_P would be justified over the whole range of particle sizes.

TABLE 1. THE VARIATION OF ANGLE OF REPOSE

Particle size cm	Region	Consolidated angle of repose
0·2435	I	43½
0·1866	I	43½
0·1340	I	43½
0·0851	I	40
0·0561	I	40
0·0358	I	40
0·0253	I	37½
0·0158	II	46½–62
0·0090	III	65½–68½
0·0071	III	90
0·0059	III	90
0·0048	III	90
0·0038	III	90

The relationships between A and D_P for regions II and III [Region I has already been dealt with (Jones & Pilpel, 1966)] are obtained by plotting A versus log D_P, giving straight lines which on regressional analyses yield

$$\text{Region II} \quad A_2 = -0{\cdot}8469 \log D_P + 0{\cdot}6182 \quad \ldots \quad (3)$$

$$\text{Region III} \quad A_3 = -4{\cdot}606 \log D_P - 6{\cdot}9213 \quad \ldots \quad \ldots \quad (4)$$

We now consider the other variable, 1/n. Log W is plotted against log D_o to give a series of straight lines obeying the well established expression

$$W \propto D_o^n \quad \ldots \quad \ldots \quad \ldots \quad \ldots \quad \ldots \quad (5)$$

The slopes of these lines (n) obtained by regression analysis are then plotted versus log D_P yielding

$$n = 0{\cdot}6927 \log D_P + 3{\cdot}6325 \quad \ldots \quad \ldots \quad (6)$$

Here a single relationship over the whole range of particle sizes is justified since the exponent term in equation (5) is an orifice function and thus not directly related to the forces between the particles. It should be noted that equation (6) yields values of 1/n which differ slightly from those obtained using the previously reported equation but is more accurate over the wider range of particle sizes now being considered.

The validity of the equation

$$D_o = A\left(\frac{4W}{60\pi\rho_P\sqrt{g}}\right)^{\frac{1}{n}}$$

where $A_1 = 1{\cdot}6822\ D_P + 1{\cdot}9779$ when $D_P > 0{\cdot}02$ cm; $A_2 = -0{\cdot}8469 \log D_P + 0{\cdot}6182$ when $0{\cdot}02 > D_P > 0{\cdot}01$ cm; $A_3 = -4{\cdot}606 \log D_P - 6{\cdot}9313$ when $0{\cdot}01 > D_P > 0{\cdot}003$ cm and $n = 0{\cdot}6927 \log D_P + 3{\cdot}6325$

for predicting the flow rates of mono systems and of binary and ternary mixtures of magnesia through different sized orifices has been tested in Tables 2, 3 and 4. The values of W_{calc} compare with the determined values (W_{obs}) to within the following accuracy: monos, mean 3%; binaries, mean 9%; ternaries, mean 8%. This is considered satisfactory.

TABLE 2. RELATIONSHIP OF W_{calc} TO W_{obs} FOR MONO-DISPERSED MATERIAL D_P <0·01 cm

D_P cm	D_o cm	W_{calc} g/min	W_{obs} g/min	Error %
0·0090	0·898	524	530–543	−1·1
	1·14	889	940–958	−5·4
0·0048	0·898	279	294–345	−5·1
	1·14	453	479–498	−5·4
0·0038	0·898	246	226–239	+2·5
	1·353	519	511–519	0

MAXIMUM FLOW

(a) *Binary systems.* Inspection of Fig. 2 shows that for binary mixtures of coarse, denoted D_{P_c}, and fine, denoted D_{P_f}, components, the flow rate attains a maximum at a definite concentration of the fine component.

The percentage of the fine component (denoted max) required to produce the maximum in the flow rate, increases with the size of the fine component and also depends upon the size of the coarse component. We have

$$\max = f(D_{P_c})(D_{P_f}) \quad .. \quad .. \quad .. \quad (7)$$

where D_{P_c} = the diameter of the coarse component and D_{P_f} = the diameter of the fine component. Now it has been shown previously (Jones & Pilpel, 1966) that in the general expression relating the flow rate of magnesia to the orifice diameter, i.e. equation (5), the exponent n is a function of the geometric mean diameter of the particles. It follows that the quantity designated max should depend on the diameter of the orifice through which the powder is flowing. Fig. 2, which is typical of a number of binary systems, shows this to be the case.

Plots of log max against D_o for binary systems yield straight line graphs showing that

$$\log \max = -mD_o + c \quad .. \quad .. \quad .. \quad (8)$$

where the negative slopes −m and the intercepts c vary with D_{P_c} and D_{P_f}. Combining equations (7) and (8) leads to the prediction that

$$\log \max = -[f(D_{P_c})(D_{P_f})]\, D_o + f(D_{P_c})(D_{P_f}) \quad .. \quad (9)$$

The data obtained in the present investigation have been used to express equation (9) explicitly the first step being to express −m and c as functions of D_{P_f} for fixed values of D_{P_c} and then to evaluate the constants of these functions in terms of D_{P_c}. We find that

$$\log \max = [X - (1061\, D_{P_c} - 118)\, D_{P_f}]\, D_o + (204 - 1506\, D_{P_c})\, D_{P_f} + Y \quad (10)$$

where $X = -3{\cdot}4854\, D_{P_c} + 0{\cdot}1887$

$Y = 14{\cdot}697\, D_{P_c} + 0{\cdot}2364$

Although this equation is empirical, it enables one to estimate the percentage of fine material that is required to produce maximum flow rate

TABLE 3. RELATIONSHIP OF W_{calc} TO W_{obs} FOR BINARY MIXTURES OF D_{P_c} to D_{P_f}

Mixture							
D_{P_c} cm	Conc % w/w	D_{P_f} cm	Conc % w/w	D_o cm	W_{calc} g/mm	W_{obs} g/mm	Error %
0·0851	80	0·0090	20	0·740	296	300–330	−1
				0·898	506	551–576	−8
				1·353	1567	1874–1871	−18
	50		50	0·740	387	398–402	−2
				0·898	635	653–690	−3
				1·353	1809	1746–1798	+1
	20		80	0·740	375	383–407	−2
				0·898	589	611–639	−8
				1·353	1516	1488–1560	0
0·0851	80	0·0071	20	0·740	304	308–315	−1
				0·898	517	537–546	−4
				1·353	1588	1763–1896	−10
	50		50	0·740	405	374–378	+7
				0·898	659	612–618	0
				1·353	1850	1776–1896	0
	20		80	0·740	373	377–392	−1
				0·898	581	596–604	−3
				1·353	1475	1440–1460	+1
0·0851	80	0·0048	20	0·740	314	318–326	−1
				0·898	530	576–585	−8
				1·353	1618	1863–1908	−11
	50		50	0·740	268	311–328	−13
				0·898	432	488–525	−11
				1·353	1183	1188–1310	0
	20		80	0·740	293	201–216	+35
				0·898	446	294–321	+39
				1·353	1090	661–672	+62
0·0561	80	0·0090	20	0·740	342	332–343	0
				0·898	571	588–595	−3
				1·353	1697	1852–1905	−8
	50		50	0·740	417	396–410	+2
				0·898	676	681–699	−1
				1·353	1880	1830–1908	0
	20		80	0·740	375	383–401	−2
				0·898	588	609–628	−3
				1·353	1526	1504–1553	0
0·0561	80	0·0071	20	0·740	348	352–357	0
				0·898	580	620–633	−6
				1·353	1713	1866–1920	−8
	50		50	0·740	435	398–412	+5
				0·898	699	635–652	+7
				1·353	1913	1572–1638	+17
	20		80	0·740	373	330–346	+8
				0·898	579	492–539	+7·4
				1·353	1467	1188–1249	+17
0·0561	80	0·0048	20	0·740	367	334–352	+4
				0·898	606	615–621	−1
				1·353	1759	1800–1960	−5
	50		50	0·740	380	339–359	+6
				0·898	605	575–611	0
				1·353	1615	1176–1193	+35
	20		80	0·740	288	174–201	+43
				0·989	439	275–294	+49
				1·353	1072	618	+73

TABLE 3—*continued*

Mixture							
D_{P_c} cm	Conc % w/w	D_{P_f} cm	Conc % w/w	D_o cm	W_{calc} g/mm	W_{obs} g/mm	Error %
0·0253	80	0·0090	20	0·740 0·898 1·353	431 695 2920	415–419 705–719 2011–2055	+ 3 − 1 +42
	50		50	0·740 0·898 1·353	378 599 1584	418–430 687–703 1776–1884	−10 −13 −11
	20		80	0·740 0·898 1·353	373 581 1475	390–394 630–641 1518–1578	− 4 − 8 − 3
0·0253	80	0·0071	20	0·740 0·898 1·353	438 703 1919	421–440 747–753 2016–2100	0 − 6 − 5
	50		50	0·740 0·898 1·353	376 591 1538	424–426 690–697 1557–1680	−11 −14 − 1
	20		80	0·740 0·898 1·353	352 541 1344	336–340 531–556 1260–1368	+ 3·5 0 0
0·0253	80	0·0048	20	0·740 0·898 1·353	449 718 1942	424–427 693–702 1968–1982	+ 5 + 2 − 1
	50		50	0·740 0·898 1·353	374 581 1475	324–340 492–522 1050–1110	+10 +11 +32
	20		80	0·740 0·898 1·353	242 365 872	228–232 345–366 663–738	+ 4 0 +18

TABLE 4. RELATIONSHIP OF W_{calc} TO W_{obs} FOR TERNARY SYSTEMS OF $D_{P_{c_1}}$–$D_{P_{c_2}}$–D_{P_f}

Mixture (% w/w)						
Size						
$D_{P_{c_1}}$ 0·0561 cm	$D_{P_{c_2}}$ 0·0253 cm	D_{P_f} 0·009 cm	D_o cm	W_{calc} g/min	W_{obs} g/min	Error %
10	20	70	0·74 0·898	374 586	418–422 678–684	−10 −14
30	30	40	0·898 1·353	630 1736	732–735 1878–1932	−14 − 8
60	20	20	0·74 1·353	363 1750	372–387 1932–2016	− 2 − 9
Size						
$D_{P_{c_1}}$ 0·0561 cm	$D_{P_{c_2}}$ 0·0253 cm	D_{P_f} 0·0048 cm				
50	40	10	0·74 1·353	368 1763	376–378 1968–2040	− 2 −10
10	10	80	0·898 0·603	394 168	356–387 170–177	+ 2 − 1
Size						
$D_{P_{c_1}}$ 0·0851 cm	$D_{P_{c_2}}$ 0·0253 cm	D_{P_f} 0·0071 cm				
70	10	20	0·898 1·14	539 1028	605–629 1158–1224	−10 −11

in binary systems with a grand mean error of 6% w/w. Allowing for the limitations of the experimental technique, this represents an error of ±10% w/w in the composition of a mixture, which is considered to be satisfactory (Table 5).

TABLE 5. COMPARISON OF MAXcalc AND MAXobs FOR BINARY MIXTURES

D_{P_c} cm	D_o cm	D_{P_f} 0·0048 cm Max$_{obs}$ % w/w	Max$_{calc}$ % w/w	Error % w/w	D_{P_f} 0·0071 cm Max$_{obs}$ % w/w	Max$_{calc}$ % w/w	Error % w/w	D_{P_f} 0·0090 cm Max$_{obs}$ % w/w	Max$_{calc}$ % w/w	Error % w/w
0·0253	0·603	20	15·9	−5	35	28·7	−5	60	46·7	−10
	0·74	20	14·3	−5	30	24·2	−5	45	37·2	−5
	0·898	10	12·8	0	25	19·8	−5	40	28·6	−10
	1·14	10	10·5	0	10	14·6	+5	20	19·2	0
	1·353	10	9·1	0	15	11·2	0	15	13·5	0
	1·686	10	6·5	0	10	7·4	0	10	7·8	0
0·0561	0·603	40	28·9	−10	60	45	−10	65	65·1	0
	0·74	35	26·4	−10	40	39·5	0	55	55·1	0
	0·898	30	23·8	−5	40	33·9	−5	45	45·4	0
	1·14	26	20·3	−5	45	26·9	−15	45	33	−10
	1·353	22	17·6	0	30	21·8	−10	30	26·1	−5
	1·686	20	14·2	−5	20	15·9	0	20	17·4	0
0·0851	0·603	40	50·2	+10	75	69·5	−5	80	89·8	+10
	0·74	35	47·1	+10	65	62·8	0	65	80·4	+15
	0·898	30	43	+10	40	56·4	+15	50	70·5	+20
	1·14	30	37·7	+10	40	47·4	+5	40	57·7	+20
	1·353	25	38·4	+15	40	41	0	40	48·3	+10
	1·686	20	27·8	+10	30	32·3	0	30	36·6	+5

(b) *Ternary systems.* Equation (10) can now be applied for predicting the percentage of fine material producing maximum flow rate in a ternary system containing two coarse, $D_{P_{c_1}}$, $D_{P_{c_2}}$, and one fine component, D_{P_f}, through any particular sized orifice.

We first construct a co-ordinate system as shown in Fig. 5. The ordinate is log max for one of the binary mixtures (say $D_{P_{c_1}}$, D_{P_f}) present

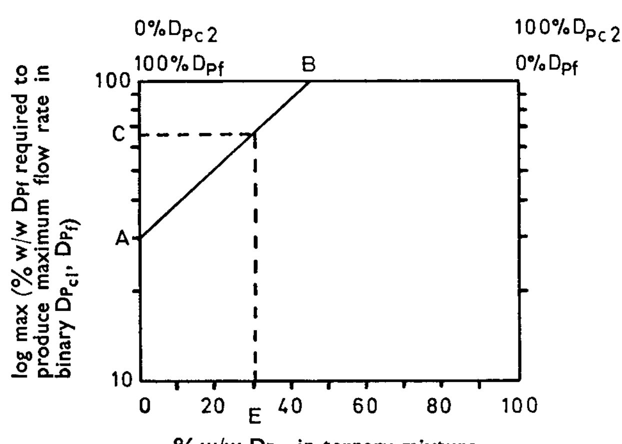

FIG. 5. Method for estimating composition for maximum flow rate in a ternary system. $D_{P_{c_1}}$ = 0·0253 cm. $D_{P_{c_2}}$ = 0·0561 cm. D_{P_f} = 0.009 cm.

in the ternary system and ranges from 1·0 representing 10% of the fine component to 2·0 representing 100% of the fine component. The abscissa expressed as % w/w of the second coarse component, $D_{P_{c_1}}$, present in the ternary system ranges from 0 to 100%. Any line emanating from the ordinate shows the variation in the amount of fine component required to produce a maximum in flow rate for the binary D_{cf} D_f in the presence of gradually increasing amounts of the third component $D_{P_{c2}}$.

Furthermore, a line drawn parallel to the abscissa through the ordinate, 2·0 (≡100% D_{P_f}) and ranging from 0% to 100% is the max of the second binary ($D_{P_{c_2}}$, D_{P_f}).

We use equation (10) to calculate max values of the two binary systems namely $D_{P_{c_1}}$, D_{P_f} and $D_{P_{c_2}}$, D_{P_f} and plot these points on the respective axes as A and B in Fig. 5.

From a straight line drawn through the points we obtain the max value for the binary $D_{P_{c_1}}$, D_{P_f}, namely the point C, on the ordinate for a particular concentration, say E% w/w of $D_{P_{c_2}}$ in the ternary system. Since the binary $D_{P_{c_1}}$, D_{P_f} represents (100 − E)% w/w of the ternary mixture, the actual concentrations (% w/w) of $D_{P_{c_1}}$ and D_{P_f} in the ternary system can be calculated.

We illustrate the procedure by an actual example. Consider the experimental data given in Fig. 4(c) which show the flow rates of ternary mixtures of 0·0090 cm (D_{P_f}), 0·0253 cm ($D_{P_{c_1}}$) and 0·0561 cm ($D_{P_{c_2}}$) particles through an orifice D_0 of 0·898 cm. The problem is to calculate the amount of D_{P_f} (% w/w) which leads to maximum flow when the ternary system contains 30% w/w of the 0·0561 cm ($D_{P_{c_2}}$) material.

We have from equation (10) that the flow rates of binary mixtures of 0·009 cm with 0·0253 cm particles and of 0·009 cm with 0·0561 cm particles are maximal when they contain respectively 30% w/w and 45% w/w of the 0·0090 cm material. In Fig 5, A = 30% w/w and is plotted on the ordinate. B = 45% w/w and is plotted on the line parallel to the abscissa at log max = 2·0. For E = 30% w/w we obtain the point C = 66% w/w D_{P_f} and the % D = (100–66) = 34% w/w. Now since $D_{P_{c_2}}$ = 30% w/w, ($D_{P_{c_1}}$ + D_{P_f}) = 70% w/w of the ternary system, and for maximum flow 66% w/w of the 70% w/w should be D_{P_f}. Therefore total D_{P_f} content = 46·2% w/w. Hence the required composition of the ternary system is % (w/w) $D_{P_{c_2}}$, 30; D_{P_f}, 46·2; $D_{P_{c_1}}$, 23·8. This is the point marked Y on Fig. 4(c), which agrees with the experimentally determined composition having maximum flow rate.

The assumption that has been made in the above treatment is that a straight line can always be drawn between the points A and B in Fig. 5. Justification for this assumption is afforded by an examination of Fig. 4 (a–d). These show the effect of composition on the flow rates of several ternary systems of 2 coarse and 1 fine component. It is seen that lines connecting the positions of the max in the binary systems (represented by two of the sides of the triangles) pass approximately through the portions of the diagrams where the flow rate is maximum. Thus the assumption seems justified.

THE MECHANISM OF FLOW RATE IMPROVEMENT—GLIDANTS

There have been two different definitions used in the past for the term glidant.

Strickland (1959), has used the term for a fine material which is added to a chemically different cohesive powder to increase its flowability and also for the fine fraction which is commonly added to a coarse granulation of the *same* material for increasing its flow rate (see also Martin, Barker & Chun, 1963).

The mechanism of action in the two instances appears to differ. In the first, the glidant is thought to separate individual powder particles and hence reduce the van der Waals' type cohesive forces which act between them (Munzel & Kagi, 1954; Craik & Miller, 1958; Strickland, 1959). In the second, the improvement is thought to be due to the glidant adhering to the surfaces of the coarser granules reducing their surface rugosity and hence their coefficient of interparticular friction (Crosby, 1960; Martin & others, 1963). Glidants can therefore be divided into (1) those reducing interparticular cohesive forces in powders; (2) those reducing surface rugosity and the coefficient of interparticular friction. Clearly in the present work dealing with the effects of fines on the flow properties of granular magnesia, we have been concerned with the second category.

The findings indicate that, although in practice, category (1) type glidants are often used, this may not always be necessary.

As the size of the fine category (2) glidant particle is increased, its ability to coat the coarser material is diminished and this reduces its efficiency. This can be seen by examining Fig. 2. The smaller the value of D_P the greater the value of max for any particular coarse second component. As the concentration of fine category (2) glidant material is increased, a point is eventually reached when its particles begin to interact with each other. This leads to a reduction in flow rate as can be seen from Figs 2 and 3.

Thus, for every real powder system there should be an optimum combination of (category 2) glidant size and concentration which leads to a maximum in the flow rate. Conversely there will be an optimum concentration of coarse material for improving the flow of a fine powder (a method that was reported by Davis, 1943, and Shotton & Simons, 1950).

Acknowledgement. One of us (T.M.J.) wishes to thank the Science Research Council for financial assistance for this work.

References

Bulsara, P. V., Zenz, F. A. & Eckert, R. A. (1964). *Ind. & Engng Chem.—Process Design & Dev.*, 3, 348–355.

Craik, D. J. & Miller, B. F. (1958). *J. Pharm. Pharmac.*, **10**, *Suppl.* 136*T*–144*T*.

Crosby, E. J. (1960). *Am. Perfumer Arom.*, **75**, 43–48.
Davis, H. (1943). *Pharm. J.*, **150**, 118.
Dawes, J. C. (1952). Safety in Mines Research Establishment Res. Rep. No. 36.
Fairs, G. L. (1960). In discussion following Brown, R. L. & Richards, J. C. (1960). *Trans. Inst. chem. Engn*, **38**, 251.
Gunsel, W. C. & Lachman, L. (1963). *J. pharm. Sci.*, **52**, 178–182.
Hammerness, F. C. & Thompson, H. O. (1958). *J. Am. pharm. Ass., Sci. Edn*, **47**, 58–61.
Hawkesley, P. G. W. (1947). *Inst. Fuel Conf. on Pulverised Coal*, 656–687.
Jenike, A. W. (1961). *Bull. Utah Engn Exp. Stn*, No. 108.
Jones, T. M. & Pilpel, N. (1966). *J. Pharm. Pharmac.*, **18**, 81–93.
Krishna, N. Gopal & Rao, M. N. (1963). *Indian Chem. Engr*, **5**, T11–T14.
Lowes, T. M. & Perry, M. C. (1965). *Rheol. Acta*, **4**, 225–166.
Martin, A. N., Barker, G. S. & Chun, A. H. C. (1964). *Advances in Pharmaceutical Science*, Vol. 1, p. 69, Editors Bean, H. S. & others. London: Academic Press.
Munzel, K. & Kagi, W. (1954). *Pharm. Acta Helv.*, **29**, 53–70.
Nakajima, E. (1961). *J. pharm. Soc. Japan*, **81**, 717–723.
Shotton, E. & Simons, F. M. (1950). *J. Pharm. Pharmac.*, **2**, 231–235.
Strickland, W. A. (1959). *Drug Cosmet. Ind.*, **85**, 318–319, 406–410.
Tucker, S. J. & Hays, H. M. (1959). *J. Am. pharm. Ass., Sci. Edn*, **48**, 362.
Vegan, N. T. (1960). *Meddr norsk. farm. Selsk.*, **22**, 153–166.